
Article:
Wang, H, Lin, G, Bai, L et al. (2 more authors) (2019) Experimental study on an acetone-charged loop heat pipe with a nickel wick. International Journal of Thermal Sciences, 146. 106104. ISSN 1290-0729

https://doi.org/10.1016/j.ijthermalsci.2019.106104

Experimental study on an acetone-charged loop heat pipe with a nickel wick

Huanfa Wang[a], Guiping Lin[a], Lizhan Bai[a,*], Jingwei Fu[a], Dongsheng Wen[a, b]

[a]Laboratory of Fundamental Science on Ergonomics and Environmental Control, School of Aeronautic Science and Engineering, Beihang University, Beijing 100191, PR China

[b]School of Chemical and Process Engineering, University of Leeds, Leeds, LS2 9JT, UK

Abstract: In order to push forward the commercial applications of loop heat pipe (LHP) especially in an environment where people are present, it is of great importance to explore alternative working fluids to substitute the commonly used anhydrous ammonia. In this work, an acetone-charged LHP with a nickel wick is developed and experimentally studied, mainly focusing on its startup and heat transport capability. Based on the experimental results and theoretical analysis, some important conclusions have been drawn, as summarized below: 1) The acetone-charged LHP with 2 mm inner diameter pipeline can successfully realize the startup, and reach a heat transport capability of 60W×0.5m; 2) When the inner diameter of the pipeline is increased from 2 to 4 mm, the LHP can start up with a much smaller heat load, i.e., 5 W, achieving a much lower steady-state operating temperature; 3) When the inner diameter of the pipeline is increased from 2 to 4 mm, the heat transport capability of the acetone-charged LHP can be increased from 60 to 100 W. 4) Adverse elevation affects greatly the heat transport capability of the acetone-charged LHP. With the adverse elevation increasing from 0 to 0.2 m, the heat transport capability is decreased from 100 to 60 W. The physical mechanisms responsible for the experimental results mentioned above have been analyzed and discussed. This work contributes to a better understanding on the operating performance and characteristics of the acetone-charged LHP, providing good design guidance and reference for its future applications.

Keywords: loop heat pipe; acetone; startup; heat transport capability; experiment

* Corresponding author. Tel.: +86 10 8233 8600; Fax: +86 10 8233 8600

E-mail address: bailizhan@buaa.edu.cn (L. Bai)

1 Introduction

As a highly efficient and reliable two-phase heat transfer device, loop heat pipe (LHP) has increasingly attracted the attention of researchers and engineers worldwide. It utilizes the evaporation and condensation phase change of a working fluid to transfer heat, and relies on the capillary forces developed in the evaporator wick to circulate the working fluid inside a closed loop where no external power is required [1-2]. Comparing with traditional heat pipes, significant structural improvements have been made for LHP, mainly including the local installment of porous wick, the employment of inverted evaporator and the separation of liquid/vapor transport lines. These structural improvements effectively overcome the inherent drawback of conventional heat pipe such as small heat transfer capacity, weak antigravity capability and unfavorable flexibility in installment, enabling LHP to be a more universal and advanced heat transfer device. Its long distance heat transport capability and flexibility in packaging as well as strong antigravity operation show obvious advantage over traditional heat pipes [3-4]. As a result, it has been widely applied in the spacecraft thermal control system to address the complicated thermal management problems during the whole mission where great success has been achieved [5-12]. With continuous development of LHP technology, its application area is gradually extended to a much wider range, such as the thermal management of aircraft and submarine [13-16], the solar thermal system [17-18] and the modern electronics cooling [19-25].

Besides the high quality wick located in the evaporator, the thermal performance of a LHP is strongly dependent on the working fluid charged inside the loop, which determines its operating temperature range, heat transport capability and heat transfer performance [26, 27]. For a LHP operating at the ambient temperature range, i.e., 0-60 ℃, anhydrous ammonia should be the best choice compared with other working fluids, only considering the heat transfer performance and heat transport capability. That is because ammonia possesses very good comprehensive thermos-physical properties, i.e., large liquid surface tension and evaporative latent heat, large vapor density, small liquid viscosity and relatively high thermal conductivity of liquid. What's more, it has very high saturation pressure difference corresponding to unit

temperature difference $(dP/dT)_{sat}$, enabling the ammonia-charged LHP to produce rather small temperature difference between the evaporator and condenser during the LHP operation, and quite favorable heat transfer performance and heat transport capability can be expected. For instance, Maydanik et al. developed and tested a stainless steel LHP with ammonia as the working fluid. The device had a transport length of 21 m, with a cylindrical evaporator 24 mm in diameter with an active zone 188 mm in length. Experimental results showed that at a cooling water temperature of 20 ℃, a maximum heat load of 1700 W was achieved at a vapor temperature of 62 ℃, corresponding to a heat source temperature of 89 ℃. Under this condition, the thermal resistance of the ‘‘heat source-cooling liquid” system was as low as 0.034 ℃/W [28]. Jasvanth et al. developed and tested a LHP with ammonia as the working fluid. The maximum heat load reached up to 600 W with an adverse elevation up to 1.0 m. For the current evaporator, the evaporative heat transfer coefficient was greater than 15,000 W/ (m^2 K) for all the cases. The evaporator thermal conductance deceased with an increase in the adverse elevation due possibly to meniscus recession into the evaporator wick. When the heat load was greater than 300 W, the LHP was operating in the constant conductance mode [29].

Although ammonia-charged LHP exhibits excellent heat transfer performance and high heat transport capability, it is generally not acceptable in commercial applications especially in an environment where people are present. That is because anhydrous ammonia is a toxic substance, which can destroy the environment and lead to serious health hazard to the people around once a fluid leakage occurs, especially in a closed finite space. In fact, the saturation pressure of ammonia at 60 ℃ is as high as 25.8 atm, and generally the risk of fluid leakage cannot be avoided absolutely. Due to the safety and health issues caused by the use of ammonia, there is an orientation to replace this substance by other working fluids of lower risk and easier to handle. To expand the application area of LHP especially in a manned environment, it is essential to explore alternative working fluids with less risk or no risk. Currently, there are two kinds of candidate working fluid that may be suitable for LHP. For one kind of working fluid, it is still toxic to some extent; however, its saturation pressure at the ambient temperature is quite close to the atmospheric pressure, even below the

atmospheric pressure, so the fluid leakage risk can be reduced significantly. Typical working fluids of this kind include acetone, methanol, ethanol, water, etc. For the other kind, although its saturation pressure at the ambient temperature may be still very high, and the leakage risk still exists, it is non-toxic and environmentally friendly. Typical working fluids of this kind are mainly Frons, such as R134a and R22.

Considering the safety and health issues for an ammonia-charged LHP, when the heat load to be dissipated is relatively small, i.e., at the level of 100-200 W, high-grade acetone becomes an interesting option for the working fluid of a LHP. Despite the lower Figure of Merit for acetone compared with ammonia, it presents several advantages such as relatively high liquid surface tension, near atmospheric pressure working pressure in the ambient temperature range, much reduced handling risks, and less expensive distillation/purification process and filling devices. It should be of note that because the working pressure of an acetone-charged LHP is very close to the atmospheric pressure, the leakage risk is considerably reduced. Accordingly, the safety concern drops to a very low degree, although acetone is either not a nonhazardous substance.

To date, relevant studies on LHPs with acetone as the working fluid, experimental or theoretical, are still quite few, as briefly reviewed below. Riehl and Bazzo compared the thermal performance of capillary pumping systems that use ammonia and acetone as the working fluids respectively. It showed that both working fluids presented close thermal performance, despite a higher superheat (temperature difference between the evaporator and compensation chamber) existed when acetone was used as the working fluid, for a reduced scale capillary evaporator [30]. Due to a relative lack of information regarding the compatibility between acetone and stainless steel, life tests for an acetone-stainless steel LHP was conducted by Riehl. The test results showed good long term interaction between acetone and stainless steel as well as outstanding thermal performance for the range of applied heat load, indicating that acetone is compatible with stainless steel [31]. Riehl and Dutra built and tested an experimental LHP with acetone as the working fluid, designed to manage up to 70 W and using a capillary evaporator with reduced active length. The experimental results showed

good thermal management performance of the proposed LHP for the imposed limitations to its design and operation. The LHP presented to be a reliable thermal management device for future space applications, especially when considering the use of a less hazardous working fluid and the particular geometric characteristics [32]. Riehl and Siqueira built and tested two loop heat pipes, where they differed from each other on their compensation chamber geometry and used high grade acetone as the working fluid, in substitution of the commonly used anhydrous ammonia. Life tests have shown reliable operation for both loop heat pipes with successful startups and continuous operation without temperature overshoot or evaporator dry-out. The life tests data has been applied on the design and construction of LHPs toward their use in future space applications [33].

Although acetone-charged LHP exhibits great potential in future commercial applications, to push forward its practical applications, comprehensive and in-depth investigations are still needed to characterize its operation and guide its design. There are still many questions for acetone-charged LHPs to be resolved. In the previous studies, the acetone-charged LHP typically used a primary wick made of UHMW polyethylene due to its much reduced thermal conductivity. The feasibility of employing a primary wick made of nickel or stainless steel powders is still unclear. The minimum heat load required to start up an acetone-charged LHP needs to be determined. In addition, how and to what extent the transport line diameter and adverse elevation may affect the heat transfer performance especially the heat transport capability of an acetone-charged LHP are still not well answered. The underlying influencing mechanisms for these factors need to be well explored and revealed. To better understand and characterize its operating performance and characteristics, and also to provide good design guidance and reference of acetone-charged LHPs, these issues mentioned above should be appropriately addressed, which forms the main objective of this work.

2 Experimental system

The LHP studied in this work was made of stainless steel except that the evaporator wick was made of sintered nickel powders. The fabrication of the nickel wick mainly included three processes in series: cold compression

moulding, sintering and precision machining. Acetone was selected as the working fluid to substitute the commonly used anhydrous ammonia. Because the saturation pressure of acetone at 56 ℃ is about 1 atm, the leakage risk for an acetone-charged LHP operating at the ambient temperature range, i.e., 0-60 ℃, can be reduced significantly. Fig. 1 shows the basic structure of a LHP, which consists of an evaporator integrated with a compensation chamber (CC), a condenser and liquid and vapor transport lines. Fig. 2 shows the detailed structure of the evaporator and CC. Table 1 provides the basic parameters of the LHP where OD and ID represent the outer and inner diameters respectively. To investigate the effect of pipeline diameter on the thermal performance of the LHP, vapor line and condenser line with 2 and 4 mm inner diameter were used respectively. Fig. 3 shows a schematic view of the experimental system. Heat load applied to the evaporator was provided by a thin-film electric resistance heater attached tightly to the outer surface of the evaporator casing, which can be adjusted in the range of 0-500 W by altering the output voltage of a DC power. The maximum uncertainty of the heat load was around ± 5.0 %. The condenser line was brazed with a copper thermal diffusion plate, and the thermal diffusion plate was then attached tightly to an aluminum cold plate. The aluminum cold plate was cooled by water with an adjustable temperature, which was circulating through a constant temperature water bath. In the experiments, all the LHP components were covered with multilayer insulation materials, to reduce the parasitic heat loss to the ambient as much as possible. Twelve type-T thermocouples with a maximum measurement error of ± 0.5 ℃ were employed to monitor the temperature profile along the loop during the tests, as illustrated in Fig. 3. Temperature data from the thermocouples was recorded, displayed and stored every five seconds by a data acquisition system 34970A linked to a PC. Different relative elevation between the evaporator and the condenser can be realized, to investigate its influence on the thermal performance especially the heat transport capability of the LHP.

3 Experimental results and analysis

3.1 Startup for LHP with 2 mm inner diameter pipeline

As the startup is the first and most important issue to be addressed prior to practical application of LHPs in both space and terrestrial surroundings, it always attracts special attention from the researchers. The startup of a LHP is a very complex dynamic process, ranging from the application of a heat load to the evaporator to the normal circulation of working fluid in the loop. During this process, a variety of heat transfer phenomena may be involved including evaporation, boiling, condensation and convection, accompanied by complicated liquid/vapor movement and phase redistribution. According to previous studies, the startup of a LHP is affected by various factors. In particular, it is strongly influenced by the initial liquid/vapor distribution in the evaporator, and four possible startup situations have been identified, as listed in Table 2. Many experiments have shown that LHPs are the easiest to start up in situation 2, but the most difficult in situation 3[34-41].

Figure 4 shows a typical startup process with a heat load of 20 W applied to the evaporator for the acetone-charged LHP with 2 mm inner diameter pipeline. In Fig. 4, the heat sink temperature was kept constant at 20 ℃, the ambient temperature was about 26 ℃, and the evaporator and condenser were placed in a horizontal plane, i.e., no adverse elevation existed. According to Fig. 4, at the initial state, all the components of the LHP were at the ambient temperature of about 26 ℃, except that the condenser temperature (TC5) was very close to the heat sink temperature of 20 ℃ due to direct contact between them. With a heat load of 20W applied to the film electric resistance heater, its temperature (TC1) together with the evaporator temperature (TC2) began to rise very quickly. At this moment, TC3 at the evaporator outlet remained almost at the ambient temperature, indicating that vapor was not immediately generated in the vapor grooves and flew into the vapor line. It was because the vapor grooves were completely flooded with liquid, and a certain liquid superheat was required to initiate the nucleate boiling there. At the same time, TC12 on the top of the CC remained at the ambient temperature, indicating that the heat leak from the evaporator to the CC was rather small under this condition. This is reasonable as the evaporator core was flooded with liquid, and the heat leak from the evaporator to the CC was mainly by the thermal conduction of the evaporator

casing and the liquid saturated wick, whose thermal resistance would be rather large. From the above temperature variations, it can be inferred that the LHP started up in situation 1.

As the evaporator temperature TC2 rose continuously, the liquid superheat increased until the onset of nucleate boiling in the vapor grooves. The film heater temperature (TC1) then dropped sharply due to the absorption of heat by liquid evaporation while the temperature at the evaporator outlet TC3 rose immediately, indicating that vapor generated in the vapor grooves was pushed out of the evaporator and then into the vapor line. At the same time, TC12 on the top of the CC began to rise at a faster rate, which should be caused by a relatively large heat leak from the evaporator. That is because at the moment of the onset of nucleate boiling, a large amount of vapor was generated in the vapor grooves, which resulted in a relatively high pressure at the outer surface of the wick. Under such a high pressure condition, some of the vapor would penetrate the porous wick and go through the evaporator core to the top region of the CC, leading to obvious increase of the heat leak from the evaporator to the CC.

The temperature at the condenser inlet (TC4) first rose sharply, approaching the temperature at the evaporator outlet (TC3) of about 60 ℃, then it dropped quickly to below 40 ℃. It showed that vapor generated in the evaporator flew into the condenser at the moment nucleate boiling occurred. However, it receded into the vapor line quickly, leading to a resultant very low utilization efficiency of the condenser. The normal circulation of working fluid in the loop could be evidenced by a step decrease of the temperature at the condenser outlet (TC10) at the moment nucleate boiling occurred. With the circulation of the working fluid in the loop, the temperatures of the evaporator and CC increased gradually until the LHP achieved the steady state operation, where the energy balance between the heat leak from the evaporator to the CC and the cooling capacity of returning subcooled liquid was reached. At the steady state, the temperatures at all the locations along the loop kept almost constant except that at some locations the temperatures maintained a slightly oscillating state, i.e., the temperatures at the condenser inlet (TC4) and at the CC inlet (TC11).

Figures 5 and 6 show the startup process of the acetone-charged LHP with a heat load of 30 and 50 W applied to the evaporator respectively. In Figs. 5 and 6, the operating conditions were all the same as those in Fig. 4 except the startup heat load. According to Figs. 5 and 6, when the heat load applied to the evaporator was 30 or 50 W, most temperature curves presented very similar variation trends to those in Fig. 4 with a heat load of 20 W. While the difference was that with the increase of the startup heat load, the vapor front in the vapor line gradually moved forward into the condenser. For example, when the startup heat load was 30 W, the temperature at the condenser inlet (TC4) rose to nearly the evaporator temperature at about 1000 s; and when the startup heat load was further increased to 50W, it rose to nearly the evaporator temperature immediately once nucleation boiling occurred in the vapor grooves.

From Figs. 4-6, when the startup heat load was 20 or 30 W, TC5 at the condenser kept almost unchanged at the moment nucleation boiling occurred; however, when the startup heat load was further increased to 50W, a small step increase of TC5 could be clearly observed, which indicated an enlarged liquid/vapor two-phase zone in the condenser and enhanced utilization efficiency of the condenser. That can well account for why the final steady-state operating temperature at the startup heat load of 50 W, i.e., 83 ℃, was obviously lower than that when the heat load was 20 or 30 W, i.e., approximately 110 ℃. It indicated that the LHP was operating in the variable conductance mode at small heat loads, an inherent and unique heat transfer characteristic for LHPs.

3.2 Heat transfer limit for LHP with 2 mm inner diameter pipeline

The heat transport capability determines the maximum heat load that the LHP evaporator can withstand. Once the heat load applied to the evaporator exceeds its maximum allowable value, the LHP will fail to operate immediately accompanied by a very sharp temperature rise, followed by a resultant failure of the thermal control task. Therefore it is really important to ensure that the heat load applied to the evaporator should be always within the maximum allowable value in practical applications, and generally a sufficient margin should be retained.

Figure 7 shows the test results of the heat transport capability of the acetone-charged LHP with 2 mm inner diameter pipeline. In Fig. 7, the operating conditions were all the same as those in Fig. 4 except the evaporator heat load. During the test, the evaporator heat load was initially set as 30W. After the evaporator temperature (TC2) achieved a stable state for at least 30 minutes, the evaporator heat load was adjusted with a 10 W step increment. As shown in Fig. 7, when the evaporator heat load was increased stepwisely from 30 to 50 W, the final steady state temperature of the evaporator kept a decreasing trend. While when the evaporator heat load was increased from 50 to 60W, it began to rise. When the evaporator heat load was further increased to 70W, the evaporator temperature rose very quickly, showing an operation failure, and the heat transport limit should be reached.

For the acetone-charged LHP investigated in this work, its heat transport capability was relatively small, i.e., only 60-70 W over a transport distance of 500 mm. For LHPs, its heat transport capability is generally caused by the capillary limit, i.e., at this critical heat load, the maximum capillary pressure provided by the evaporator wick is just equal to the total pressure drop along the entire loop including the pressure drops in the vapor groove, vapor line, condenser, liquid line and evaporator wick as well as the pressure drop/gain due to the gravity effect, as shown by equation (1):

$$\Delta P_{cap,\max} = \Delta P_{vg} + \Delta P_{vl} + \Delta P_{cond} + \Delta P_{ll} + \Delta P_{wi} \pm \Delta P_{g} \quad (1)$$

Because the acetone-charged LHP here used 2 mm inner diameter pipeline, the pressure drop in the transport lines especially in the vapor line and condenser was relatively large. For instance, when the heat load is 100W at an operating temperature of 60 ℃, the pressure drop in the vapor line can reach as much as 12 kPa/m. In addition, as the effective pore radius of the evaporator wick was very small, the pressure drop in the evaporator wick was also very large. Based on our calculation, when the heat load is 100 W at an operating temperature of 60 ℃, the pressure drop in the evaporator wick can reach approximately 40 kPa corresponding to the current wick structure, according to Darcy's law for fluid flow in the porous structure.

The small heat transport capability of the acetone-charged LHP should be attributed to both its structural parameters of the LHP and the thermo-physical properties of acetone. Because the pressures drops in the vapor line, condenser and evaporator wick are relatively large based on our simple calculation and years of research experience, the structural parameters for these components should be optimized in future design of the acetone-charged LHP. Since it would cost a long time to design, manufacture and assemble a new evaporator with optimized parameters, currently we first changed the inner diameter of the vapor line and the condenser line, to investigate its influence on the startup and heat transport capability of the acetone-charged LHP, as reported in detail below.

3.3 Startup for LHP with 4 mm inner diameter pipeline

Figures 8-10 show the startup process with a heat load of 5, 10 and 20 W applied to the evaporator respectively, for the acetone-charged LHP with 4mm inner diameter pipeline. In Figs. 8-10, the operating conditions were all the same as those in Fig. 4, i.e., the heat sink temperature was kept constant at 20 ℃, the ambient temperature was about 26 ℃, and the evaporator and condenser were placed in a horizontal plane.

According to Figs. 8-10, when the heat load applied to the evaporator was 5, 10 or 20 W, most temperature curves corresponding to the characteristic points along the loop presented very similar variation trends to those in Figs. 4-6. In Ref. [32], the startup of an acetone-charged LHP with a polyethylene wick was experimentally studied, and it was found that the LHP could start up at a small heat load of 5 W, reaching a steady state operating temperature of about 35.6 ℃. Comparing with the results in Ref. [32], the operating temperature of the LHP at a heat load of 5 W in this work was obviously much higher. There are mainly two reasons responsible for this result: first, the heat sink temperature in this work, i.e., 20 ℃, is much higher than that in Ref. [32], i.e., -5 ℃; second, the radial thermal conductance of the nickel wick in this work is much larger than that of the polyethylene one in Ref. [32], leading to significantly enhanced heat leak from the evaporator to the CC.

Comparing the startup processes in Figs. 8-10 with those in Figs. 4-6, two obvious differences were quite

impressive: first, the sharp angle on the temperature curves of the film heater during the startup process disappeared for the LHP with 4mm inner diameter pipeline; second, the final steady state operating temperature of the evaporator decreased considerably for the LHP with 4mm inner diameter pipeline. In this work, the startup processes with an evaporator heat load of 5 and 10 W were not provided for the LHP with 2 mm inner diameter pipeline, because the final steady state operating temperature of the evaporator was so high that it would cause the burn-out of the film heater. Hence in the experiment for safety consideration, the startup was terminated before it reached the steady state.

These changes are closely associated with the increased inner diameter of the vapor line and the condenser line. When the inner diameter of the vapor line and the condenser line is increased from 2 to 4 mm, the pressure drops in these components can be reduced considerably, leading to a much smaller total pressure drop in the external loop. Based on the Clausius-Clapeyron equation, the saturation temperature difference between the evaporator and the CC can be calculated by equation (2):

$$\Delta T_{\text{sat,e-cc}} = \left(\frac{\mathrm{d}T}{\mathrm{d}P}\right)_{\text{sat}} \times \Delta P_{\text{ext}} = \frac{T_{\text{sat}} v_{\text{fg}}}{h_{\text{fg}}} \times \Delta P_{\text{ext}} \tag{2}$$

where T_{sat} is the saturation temperature of vapor; v_{fg} is the difference of the specific volume between saturated vapor and liquid; h_{fg} is the latent heat of vaporization and ΔP_{ext} is the pressure drop in the external loop.

According to equation (2), the larger the pressure drop in the external loop, the greater the saturation temperature difference between the evaporator and the CC. Meanwhile, for acetone at the ambient temperature range, comparing with ammonia, its saturation pressure difference corresponding to unit temperature difference becomes much smaller, making the saturation temperature difference between the evaporator and the CC to be more sensitive to the change of the pressure drop in the external loop. The reduction in the pressure drop in the external loop causes a decrease in the saturation temperature difference between the evaporator and the CC, resulting in an obviously reduced heat leak from the evaporator to the CC. With the decrease of the heat leak from the evaporator to the CC,

the required subcooling capacity of the returning liquid is reduced, a higher utilization efficiency of the condenser can be achieved, and under this condition the LHP can operate at a much lower temperature level, as evidenced by Figs. 8-10.

In addition, with the increase of the inner diameter of the vapor line and the condenser line, the vapor front enters the condenser more easily. For example, when the inner diameter of the vapor line and the condenser line was 2 mm, the vapor front began to enter the condenser at an evaporator heat load of 30 W, evidenced by the temperature at the condenser inlet (TC4) approaching closely to the evaporator temperature. When the inner diameter of the vapor line and the condenser line was increased to 4mm, the vapor front began to enter the condenser at a much lower evaporator heat load of 10 W, as shown in Fig. 9. This results is consistent with the decrease of the operating temperature of the LHP. Because once vapor generated in the evaporator enters the condenser, the heat load applied to the evaporator can be transferred efficiently to the heat sink, generating a more efficient heat transfer system.

3.4 Heat transfer limit for LHP with 4 mm inner diameter pipeline

3.4.1 Operation under horizontal orientation

Figure 11 shows the test results of the heat transport capability of the acetone-charged LHP with 4 mm inner diameter pipeline. In Fig. 11, the operating conditions were all the same as those in Fig. 7 except the inner diameter of the vapor line and the condenser line. During the test, the evaporator heat load was initially set as 20W. After the evaporator temperature (TC2) achieved a stable state for at least 30 minutes, the evaporator heat load was adjusted with a 20 W step increment. As shown in Fig. 11, when the evaporator heat load was increased stepwisely from 20 to 100 W, the final steady state temperature of the evaporator always kept a slightly increasing trend, just contrary to the case in Fig. 7. When the evaporator heat load was further increased to 110 W, the evaporator temperature rose very quickly, suggesting an operation failure, and the heat transport limit should be reached. In Ref. [32], the heat transport capability of the acetone-charged LHP with a polyethylene wick could reach 70W×0.8m. While in this

work, the acetone-charged LHP with a nickel wick can achieve a heat transport capability of about 100W×0.5m. Through simple comparison, the heat transport capability of an acetone-charged LHP with a nickel wick can be comparable to that with a polyethylene wick.

Comparing Fig. 11 with Fig. 7, it is found that the inner diameter of the vapor line and the condenser line imposes a significant effect on the heat transport limit of the acetone-charged LHP. When the inner diameter was increased from 2 to 4 mm, the heat transport limit could be enhanced obviously from 60 to 100 W. This obvious enhancement is caused by a larger inner diameter, but what is the underlying influencing mechanism? Someone may think it is directly due to a reduction in the pressure drop along the external loop. In fact, at a heat load of 60 W with an operating temperature of 92 ℃, when the inner diameter of the vapor line and the condenser line was increased from 2 to 4 mm, the pressure reduction along the external loop was less than 0.6 kPa through our careful calculation. This pressure reduction is rather small and can be almost neglected comparing to the maximum capillary pressure of about 60 kPa, which is not likely to result in such an obvious enhancement in the heat transport limit. Based on the theoretical analysis, the authors think this enhancement should be mainly due to the decrease of the operating temperature, which can produce a significant influence on the heat transport limit.

Typically, there are two combined parameters to characterize the heat transport limit for a working fluid employed in a LHP, i.e., the Dunbar parameter and the Figure of Merit [42-45], as expressed by equations (3) and (4) respectively:

$$Du = \frac{\lambda^{1.75}\sigma\rho_v}{\mu_v^{0.25}} \tag{3}$$

$$K_l = \frac{\rho_l\sigma\lambda}{\mu_l} \tag{4}$$

The greater the Dunbar parameter or the Figure of Merit, the larger the heat transport limit of the LHP charged with that working fluid. It should be of note that the two parameters are applicable to different situations: the Dunbar

parameter is used when the pressure drop for the vapor phase such as in the vapor line and condenser dominates the total pressure drop in the system; while the Figure of Merit is adopted when the pressure drop in the liquid phase such as in the evaporator wick dominates the total pressure drop. In rare conditions, if the pressure drop in the vapor phase is comparable to that in the liquid phase, the Dunbar parameter and the Figure of Merit should be both considered. In this work, according to our calculation, the pressure drop in the evaporator wick dominates the total pressure drop, so the Figure of Merit is applied here to analyze the effect of operating temperature on the heat transport limit. Fig. 12 shows the temperature dependence of the Figure of Merit of liquid acetone. As shown in Fig. 12, with the decrease of the temperature, the Figure of Merit of liquid acetone increases obviously. To be specific, the Figure of Merit increases from 25.5×10^9 kg/s^3 at the temperature of 97 ℃ to 29.4×10^9 kg/s^3 at the temperature of 73 ℃, which should be responsible for the significantly enhanced heat transport limit for the acetone-charged LHP.

3.4.2 Operation with adverse elevation

Figures 13 and 14 show the test results of the heat transport capability of the acetone-charged LHP with 4 mm inner diameter pipeline with 0.1 and 0.2 m adverse elevations respectively. In Figs. 13 and 14, the operating conditions were all the same as those in Fig. 11 except the adverse elevation. During the test, the evaporator heat load was initially set as 20 W. After the evaporator temperature (TC2) achieved a stable state for at least 30 minutes, the evaporator heat load was adjusted with a 20 W step increment.

As shown in Fig. 13, with an adverse elevation of 0.1m, the heat load dependence of the LHP operating temperature seems irregular. When the evaporator heat load was increased from 20 to 40 W, the final steady state temperature of the evaporator first increased. When the heat load was increased from 40 to 60 W, the operating temperature dropped to a lower value with a slightly oscillating state. With the heat load increasing from 60 to 80 W, the operating temperature increased again. When the evaporator heat load was further increased to 100 W, the

evaporator temperature rose very quickly, indicating an operation failure, and the heat transport limit should be reached.

According to Fig. 14, with an adverse elevation of 0.2 m, when the evaporator heat load was increased from 20 to 40 W, the final steady state temperature of the evaporator first decreased. When the heat load was increased from 40 to 60 W, the operating temperature kept almost unchanged. When the evaporator heat load was further increased to 80 W, a quick temperature rise for the evaporator was observed, showing an operation failure and the heat transport limit.

Comparing Figs.13 and 14 with Fig. 11, it is found that the adverse elevation also imposes an important effect on the heat transport limit of the acetone-charged LHP. With no adverse elevation, the LHP had a heat transport limit of 100 W. However, with an adverse elevation of 0.1 and 0.2 m, its heat transport limit was reduce to about 80 and 60 W respectively. The influencing mechanism for the adverse elevation can be analyzed below. The existence of adverse elevation will lead to an additional pressure drop in the external loop, i.e., the gravitational pressure drop as expressed by equation (5):

$$\Delta P_g = \left(\rho_l - \rho_v\right) g \Delta H \tag{5}$$

According to equation (5), the larger the adverse elevation, the greater the gravitational pressure drop. An adverse elevation of 0.1 and 0.2 m corresponds to an additional gravitational pressure drop of 0.7 and 1.4 kPa respectively. In fact, comparing with the maximum capillary pressure the evaporator wick can provide, i.e., ~ 60 kPa, the gravitational pressure drop with an adverse elevation of 0.1 or 0.2 m is rather small, which can be generally neglected. Therefore the obviously reduced heat transport limit of the LHP should not be directly caused by an increase of the pressure drop in the external loop due to the existence of adverse elevation. In the authors' understanding, the influencing mechanism for the adverse elevation on the heat transport limit is quite similar to that of the pipe inner diameter.

The presence of adverse elevation results in an additional pressure drop in the external loop, leading to enlarged saturation temperature difference between the evaporator and the CC according to equation (2). Under this condition, the heat leak from the evaporator to the CC increases accordingly, causing an increase of the operating temperature. The larger the adverse elevation, the higher the operating temperature of the LHP. For example, with a heat load of 40W applied to the evaporator, the LHP reached a final steady state operating temperature of about 62 ℃; however, the operating temperature increased to up to nearly 90℃ with an adverse elevation of 0.1m. As shown in Fig. 12, the operating temperature increase will lead to a decrease of the Figure of Merit of liquid acetone, which should be responsible for the decrease of the heat transport limit of the acetone-charged LHP.

4 Discussions

This work validated experimentally the feasibility of employing a nickel wick for an acetone-charged LHP although the radial thermal conductance of the wick becomes much larger than that of a polyethylene wick. It was identified that the heat transfer capability of the acetone-charged LHP in this work should be mainly dependent on the Figure of Merit of liquid acetone rather than the Dunbar parameter. The underlying mechanisms responsible for the effects of pipeline inner diameter and adverse elevation on the thermal performance of the acetone-charged LHP were theoretically analyzed. The experimental results obtained in this work contribute to a better understanding on the operating performance and characteristics of the acetone-charged LHP, and can provide good design guidance and reference for the future practical applications of LHPs with acetone as the working fluid. However, in order to push forward the future applications of acetone-charged LHP, its thermal performance especially in the following two aspects should be further improved significantly: decreasing the operating temperature and increasing the heat transfer limit. For most electronic devices, the maximum allowable operating temperature is usually limited by 75 or 80 ℃. For the current acetone-charged LHP with 4 mm inner diameter transport line, its steady-state operating temperature is quite close to 75 ℃ at a heat load of 100 W, which should be further lowered to fulfill the cooling

task. In addition, modern electronic and telecommunication devices are developing in the trends of miniaturization and high power, and the heat required to be dissipated is becoming large and large. Under this condition, the heat transport capability of the current acetone-charged LHP is obviously insufficient, and a notable enhancement must be achieved. To meet future application requirements, a feasible solution should be mainly focused on the structural parameter optimization of the evaporator wick, in both the macroscopic scale such as the diameter and thickness of the wick and the microscopic scale such as the effective pore radius and porosity of the wick. Moreover, the heat transfer area of the condenser should be enlarged accordingly.

5 Conclusions

In this work, extensive experimental studies on an acetone-charged LHP with a nickel wick were carried out, mainly focusing on its startup and heat transport capability. Based on the experimental results and theoretical analysis, some specific conclusions have been drawn, as summarized below:

- The acetone-charged LHP with 2 mm inner diameter pipeline can successfully realize the startup, and reach a heat transport capability of about 60W×0.5m.
- In most cases, the acetone-charged LHP starts up with the vapor grooves and evaporator core fully filled with liquid. When the inner diameter of the pipeline is increased from 2 to 4 mm, the LHP can start up at a much smaller heat load, i.e., 5 W, reaching a much lower steady-state operating temperature, because the vapor generated in the evaporator can enter the condenser more easily, resulting in an enhanced utilization efficiency of the condenser.
- The inner diameter of the vapor line and condenser line affects greatly the heat transport capability of the acetone-charged LHP. When the inner diameter is increased from 2 to 4 mm, the heat transport capability of the LHP can be increased from 60 to 100 W.
- The adverse elevation plays an important role in the heat transport capability of the acetone-charged LHP. With

the adverse elevation increasing from 0 to 0.2 m, the heat transport capability for the acetone-charged LHP with 4 mm inner diameter pipeline is decreased from 100 to 60 W.

- The influencing mechanisms of the pipeline inner diameter and adverse elevation on the heat transport limit of the acetone-charged LHP are theoretically analyzed, and the highly temperature-dependent Figure of Merit of liquid acetone plays an import role in the heat transport limit.

Acknowledgements

This work was supported by the Beijing Natural Science Foundation (No. 3182023), and the National Natural Science Foundation of China (Nos. 51576010 and 51776012).

Nomenclature

Du	Dunbar parameter	$W^{1.75}$
H	elevation	m
K	Figure of Merit	W/m^2
P	pressure	Pa
T	temperature	℃

Greek symbols

ρ	density	kg/m^3
σ	surface tension	N/m
μ	dynamic viscosity	Pa·s
λ	evaporative latent heat	J/kg

Subscripts

cap	capillary
cond	condenser
e-cc	evaporator and CC
ext	external
fg	vapor and liquid
g	gravity
l	liquid
ll	liquid line
max	maximum
sat	saturation
v	vapor
vg	vapor groove
vl	vapor line
wi	wick

References

[1] Y. F. Maydanik, Loop heat pipes, Applied Thermal Engineering, 25 (2005) 635-657

[2] J. Ku, Operating Characteristics of Loop Heat Pipes, SAE Paper, No. 1999-01-2007, 1999

[3] M. Khalili, A. Mostafazade Abolmaali, M. B. Shafii, Experimental and analytical study of thermohydraulic performance of a novel loop heat pipe with an innovative active temperature control method, Applied Thermal Engineering, 143(2018) 964-976

[4] S. Launay, V. Sartre, J. Bonjour, Parametric analysis of loop heat pipe operation: a literature review, International Journal of Thermal Sciences, 46(7) (2007) 621-636

[5] T.D. Swanson, G.C. Biru, NASA thermal control technologies for robotic spacecraft. Applied Thermal Engineering, 23(2003): 1055-1065

[6] K. Goncharov, O. Golovin, V. Kolesnikov, et al., Development and flight operation of LHP used for cooling nickel-cadmium batteries in Chinese meteorological satellites FY-1, Proc. 13th Int. Heat Pipe Conf., Shanghai, China, 2004

[7] K. Nakamura, K. Odagiri, Hosei Nagano, Study on a loop heat pipe for a long-distance heat transport under anti-gravity condition, Applied Thermal Engineering 107(2016)167–174

[8] L. Mottet, M. Prat, Numerical simulation of heat and mass transfer in bidispersed capillary structures: Application to the evaporator of a loop heat pipe, Applied Thermal Engineering 102 (2016) 770–784

[9] J. Esarte, A. Bernardini, J.M. Blanco, et al., Optimizing the design for a two-phase cooling loop heat pipe: Part A: Numerical model, validation and application to a case study, Applied Thermal Engineering 99 (2016) 892–904

[10] Triem T. Hoang, William J. Armiger, Robert W. Baldauff, et al., Performance of COMMx loop heat pipe on TacSat 4 spacecraf, AIAA Paper, No. 2012-3498, 2012

[11] D. Mishkinis, G. Wang, D. Nikanpour, et al., Advances in two-phase loop with capillary pump technology and space applications, SAE Paper, No. 2005-01-2883, 2005

[12] J. Ku, S. Jeong, D. Butler, Testing of a miniature loop heat pipe using a thermal electrical cooler for temperature control, SAE

paper, No. 2004-01-2505, 2004

[13] Y. Xie, J. Zhang, L. Xie, et al., Experimental investigation on the operating characteristics of a dual compensation chamber loop heat pipe subjected to acceleration field, Applied Thermal Engineering 81(2015) 297–312

[14] Y. Xie, Y. Zhou, D. Wen, et al., Experimental investigation on transient characteristics of a dual compensation chamber loop heat pipe subjected to acceleration forces, Applied Thermal Engineering 130 (2018) 169-184

[15] Lizhan Bai, Guiping Lin, Dongsheng Wen, et al., Experimental investigation of startup behaviors of a dual compensation chamber loop heat pipe with insufficient fluid inventory, Applied Thermal Engineering 29(2009)1447-1456

[16] G.P. Lin, H.X. Zhang, X.G. Shao, et al., Development and Test Results of a Dual Compensation Chamber Loop Heat Pipe. Journal of Thermophysics and Heat Transfer, 20(4)(2006): 825-834

[17] X.X. Zhang, X.D. Zhao, J.C. Shen, et al., Dynamic performance of a novel solar photovoltaic/loop-heat-pipe heat pump system. Applied Energy 114(2014): 335–352

[18] X.X. Zhang, X.D. Zhao, J.H. Xu, et al., Characterization of a solar photovoltaic/loop heat pipe heat pump water heating system. Applied Energy 102(2013):1229–1245

[19] Jiang He, Guiping Lin, Lizhan Bai, et al., Effect of non-condensable gas on the operation of a loop heat pipe. International Journal of Heat and Mass Transfer 70(2014) 449-462

[20] Jiang He, Guiping Lin, Lizhan Bai, et al., Effect of non-condensable gas on steady-state operation of a loop thermosyphon. International Journal of Thermal Sciences 81(2014) 59-67

[21] V.G. Pastukhov, Y.F. Maydanik, Low-noise cooling system for PC on the base of loop heat pipes. Applied Thermal Engineering 27(2007): 894–901

[22] L. Vasiliev, D. Lossouarn, C. Romestant, et al., Loop heat pipe for cooling of high-power electronic components. International Journal of Heat and Mass Transfer 52(2009): 301–308

[23] J. Li, D.M. Wang, G.P. Peterson, Experimental studies on a high performance compact loop heat pipe with a square flat evaporator.

Applied Thermal Engineering 30(2010): 741–752

[24] Z.P. Wan, X.W. Wang, Y. Tang, Condenser design optimization and operation characteristics of a novel miniature loop heat pipe. Energy Conversion and Management 64(2012): 35–42

[25] G.H. Zhou, J. Li, L.C. Lv, An ultra-thin miniature loop heat pipe cooler for mobile electronics. Applied Thermal Engineering 109(2016): 514–523.

[26] D. Reay, P. Kew, Heat Pipes Theory, Design and Applications, Fifth Ed., Burlington: Butterworth-Heinemann, 2006

[27] P.D. Dunn, D.A. Reay, Heat Pipes, Pergamon, London, 1994

[28] Y. Maydanik, V. Pastukhov, M. Chernysheva, Development and investigation of a loop heat pipe with a high heat-transfer capacity, Applied Thermal Engineering 130 (2018) 1052-1061

[29] V.S. Jasvanth, Abhijit A. Adoni, V. Jaikumar, et al., Design and testing of an ammonia loop heat pipe, Applied Thermal Engineering 111 (2017) 1655-1663

[30] R. R. Riehl, E. Bazzo, Comparison between acetone and ammonia on the thermal performance of a small-scale capillary pumped two-phase loop. Space Technology and Applications International Forum (STAIF-2003), American Institute of Physics Conference Proceedings, Albuquerque, NM, 654 (1) (2003) 80-87

[31] R. R. Riehl, Comparing the behavior of a loop heat pipe with different elevations of the capillary evaporator, 34th International Conference on Environmental Systems, Colorado Springs, CO, July 19-22, paper 2004-01-2510, 2004

[32] R.R. Riehl, T. Dutra, Development of an experimental loop heat pipe for application in future space missions, Appl. Therm. Eng. 25 (2005) 101–112

[33] R.R. Riehl, T.C.P.A Siqueira, Heat transport capability and compensation chamber influence in loop heat pipes performance, App. Therm. Eng. 26 (2006) 1158–1168

[34] Wukchul Joung, Taeu Yu, Jinho Lee, Experimental study on the operating characteristics of a flat bifacial evaporator loop heat pipe, International Journal of Heat and Mass Transfer 53(2010) 276–285

[35] Randeep Singh, Aliakbar Akbarzadeh, Masataka Mochizuki, Operational characteristics of the miniature loop heat pipe with non-condensable gases, International Journal of Heat and Mass Transfer 53(2010) 3471–3482

[36] M. N. Nikitkin, W. B. Bienert, K. A. Goncharov, Non-condensable gases and loop heat pipe operation, SAE Paper, No. 981584,1998

[37] Kimberly R. Wrenn, David A. Wolf, Edward J. Kroliczek, Effect of noncondensible gas and evaporator mass on loop heat pipe performance. SAE Paper, No. 2000-01-2409, 2000

[38] H. X. Zhang, G. P. Lin, T. Ding, et al, Investigation of startup behaviors of a loop heat pipe, Journal of Thermophysics and Heat Transfer, 19(4)(2005) 509-518

[39] T. T. Hoang, R. W. Baldauff, K. H. Cheung, Start-up behavior of an ammonia loop heat pipe, AIAA paper, No. 2005-5630

[40] Xianfeng Zhang, Jiepeng Huo, Shuangfeng Wang. Experimental investigation on temperature oscillation in a miniature loop heat pipe with flat evaporator. Experimental Thermal and Fluid Science 37 (2012) 29–36

[41] Yuming Chen, Manfred Groll, Rainer Mertz, et al. Steady-state and transient performance of a miniature loop heat pipe. International Journal of Thermal Sciences 45 (2006) 1084–1090

[42] Qian Su, Shinan Chang, Yuanyuan Zhao, et al., A review of loop heat pipes for aircraft anti-icing applications, Applied Thermal Engineering 130 (2018) 528-540

[43] Trijo Tharayil, Lazarus Godson Asirvatham, Vysakh Ravindran, et al., Effect of filling ratio on the performance of a novel miniature loop heat pipe having different diameter transport lines, Applied Thermal Engineering 106 (2016) 588-600

[44] Randeep Singh, Aliakbar Akbarzadeh Chris Dixon, Masataka Mochizuki, Novel Design of a Miniature Loop Heat Pipe Evaporator for Electronic Cooling, Journal of Heat Transfer, 129 (2007) 1445-1452

[45] Wukchul Joung, Jinho Lee, Sanghyun Lee, et al., Derivation and Validation of a Figure of Merit for Loop Heat Pipes With Medium Temperature Working Fluids, Journal of Heat Transfer, 138 (2016) , paper No. 052901

Table captions

Table 1 Basic parameters of the tested LHP

Table 2 Liquid/vapor distribution in the evaporator

Figure captions

Table 1 Basic parameters of the tested LHP

Components	Parameters
OD/ID×Length of evaporator casing/mm	18/16×130
OD/ID×Length of wick/mm	16/5×100
OD/ID×Length of vapor line/mm	3/2×500; 6/4×500
OD/ID×Length of condenser/mm	3/2×1600; 6/4×300
OD/ID×Length of liquid line/mm	3/2×500
Number×height×width of Grooves/mm	8×1×1
Volume of CC /ml	24.6
Working fluid inventory/g	28.2
Porosity of wick	55.0%
Maximum pore radius of wick/μm	0.53

Table 2 Liquid/vapor distribution in the evaporator

Situations	Vapor grooves/evaporator core
1	Liquid filled/liquid filled
2	Vapor exists/ liquid filled
3	Liquid filled /vapor exists
4	Vapor exists/vapor exists

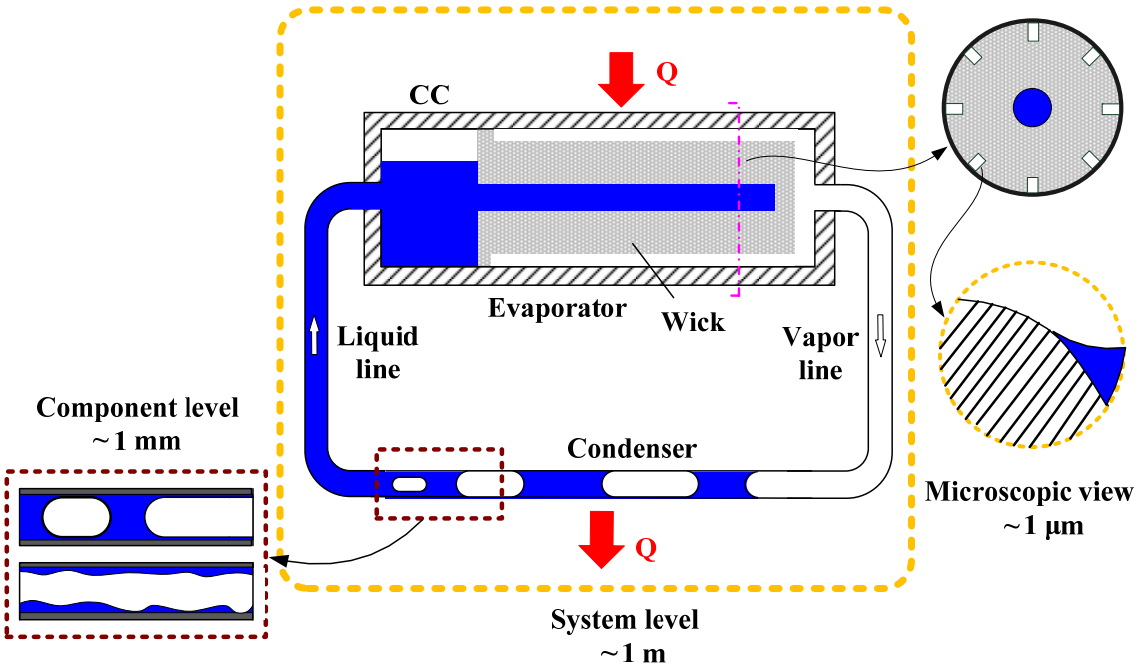

Fig. 1 Basic structure of a loop heat pipe

(a) Photo of the evaporator and compensation chamber

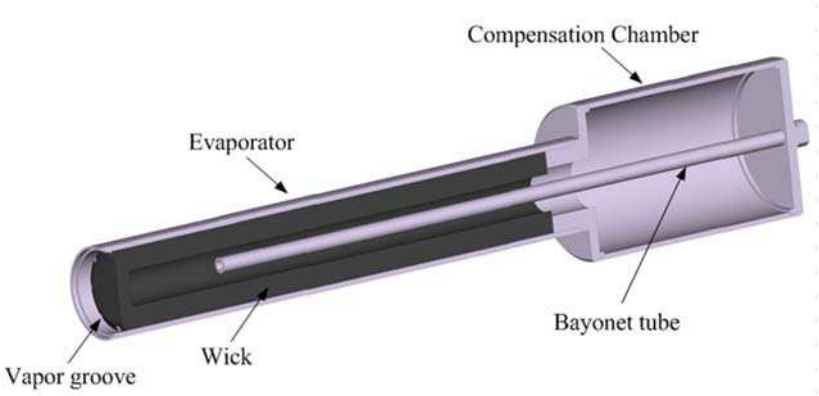

(b) Internal structure of the evaporator and compensation chamber

Fig. 2 Structure of the evaporator and compensation chamber

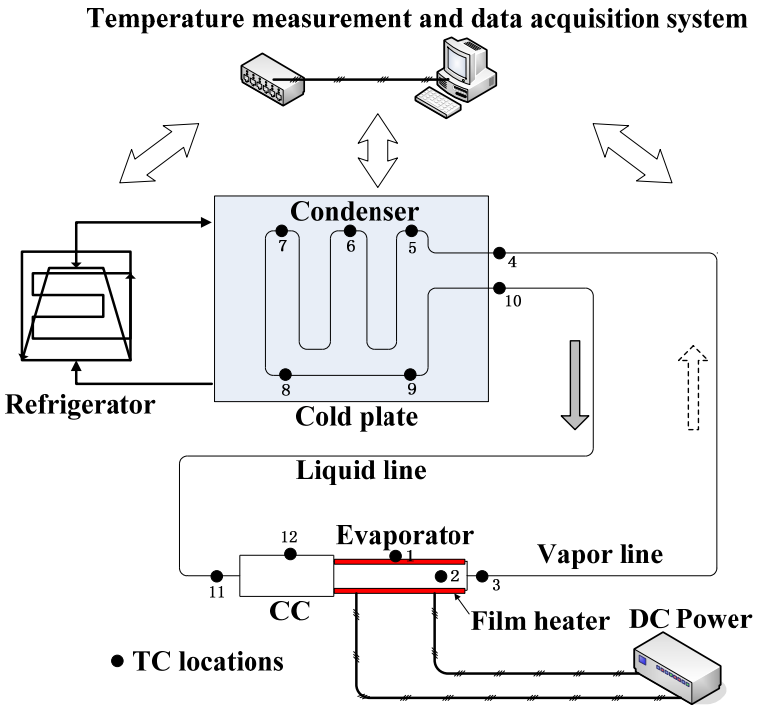

Fig. 3 Schematic of the experimental system and thermocouple locations

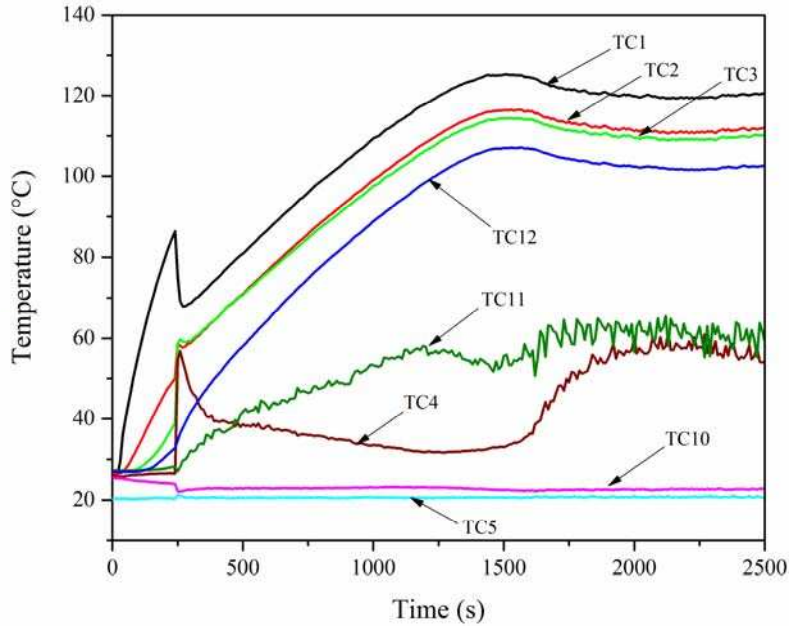

Fig. 4 Startup with a heat load of 20 W for LHP with 2 mm inner diameter pipeline

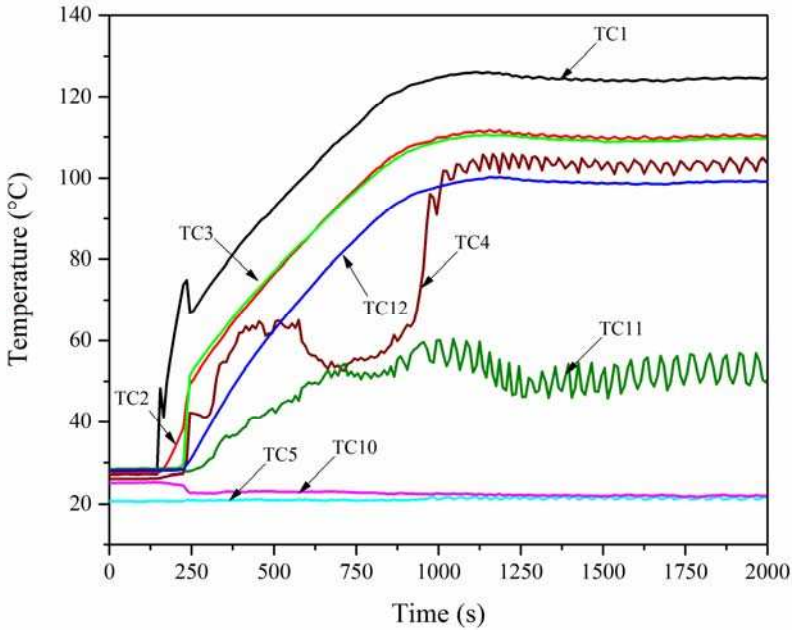

Fig. 5 Startup with a heat load of 30 W for LHP with 2 mm inner diameter pipeline

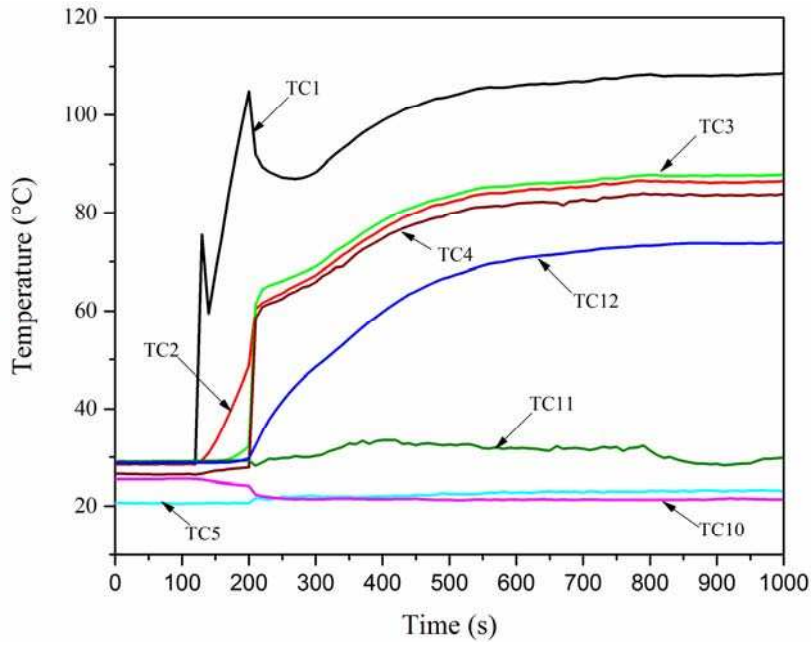

Fig. 6 Startup with a heat load of 50 W for LHP with 2 mm inner diameter pipeline

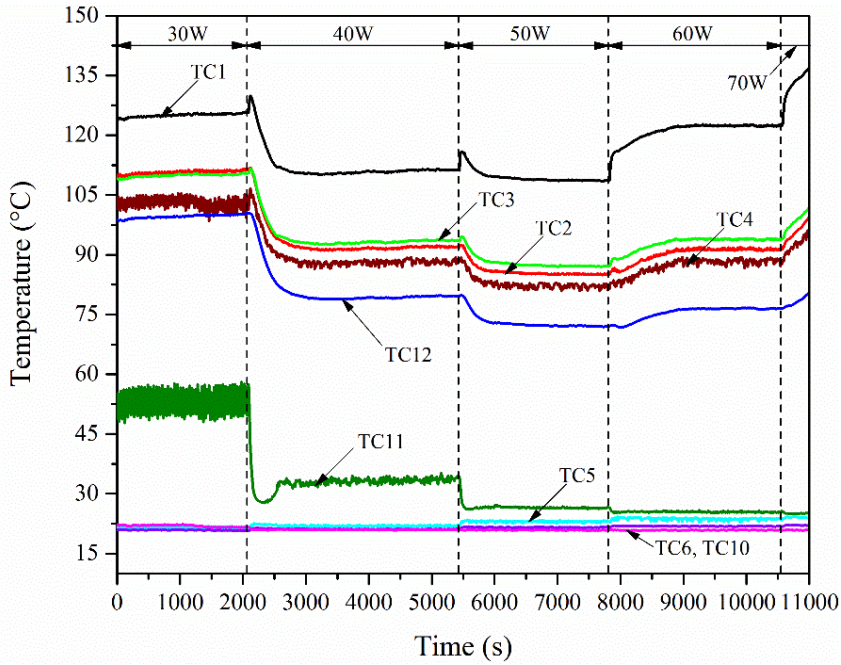

Fig. 7 Heat transfer limit for LHP with 2 mm inner diameter pipeline

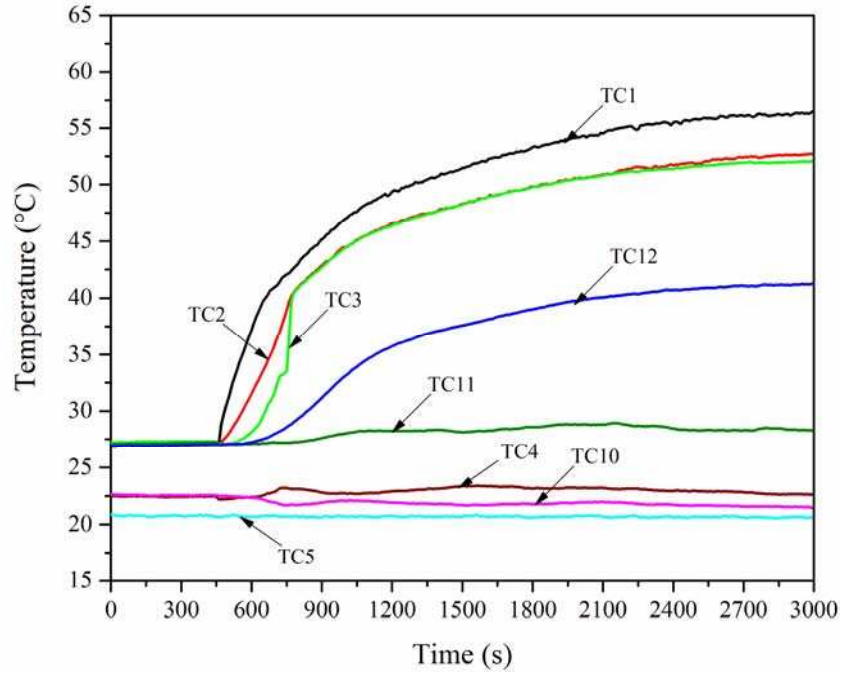

Fig. 8 Startup with a heat load of 5 W for LHP with 4 mm inner diameter pipeline

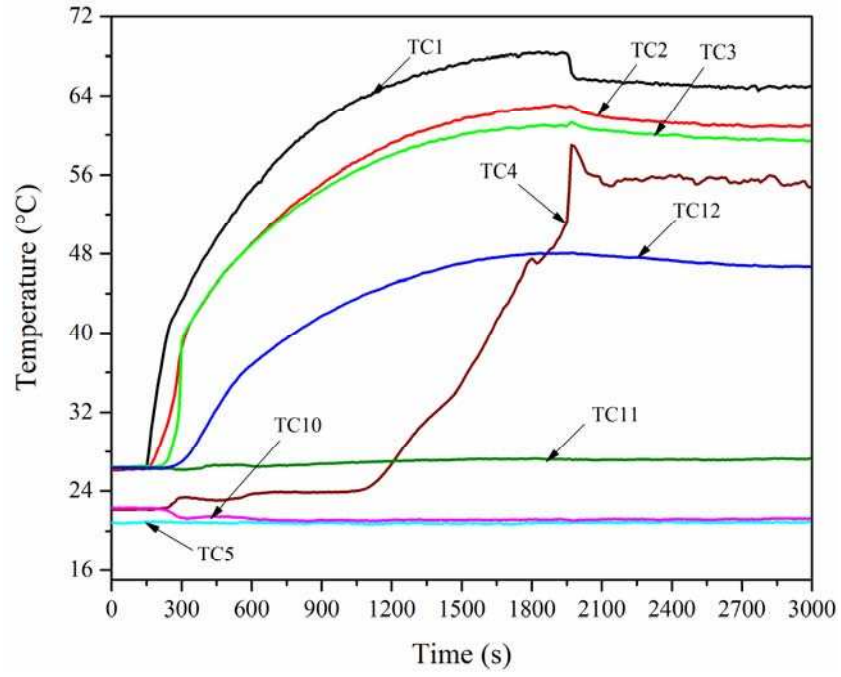

Fig. 9 Startup with a heat load of 10 W for LHP with 4 mm inner diameter pipeline

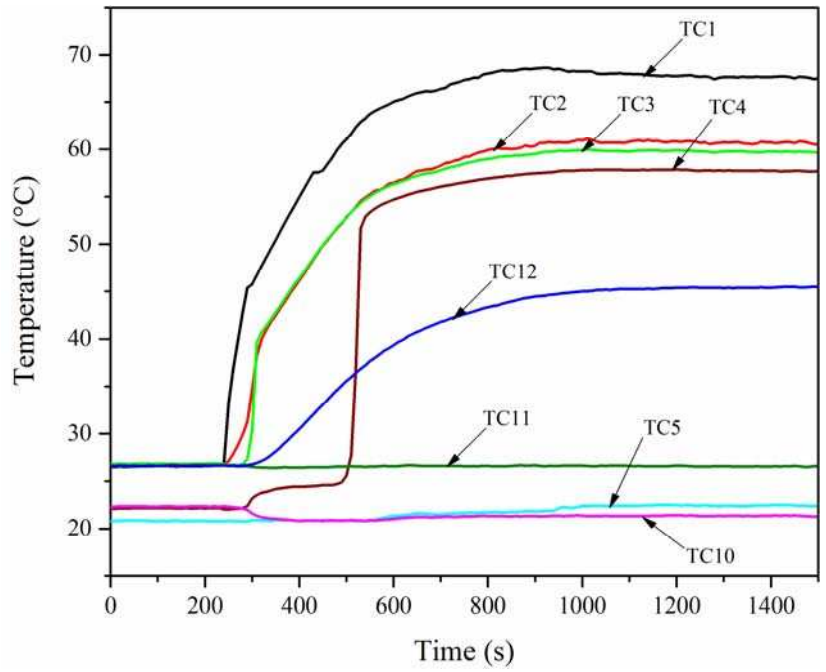

Fig. 10 Startup with a heat load of 20 W for LHP with 4 mm inner diameter pipeline

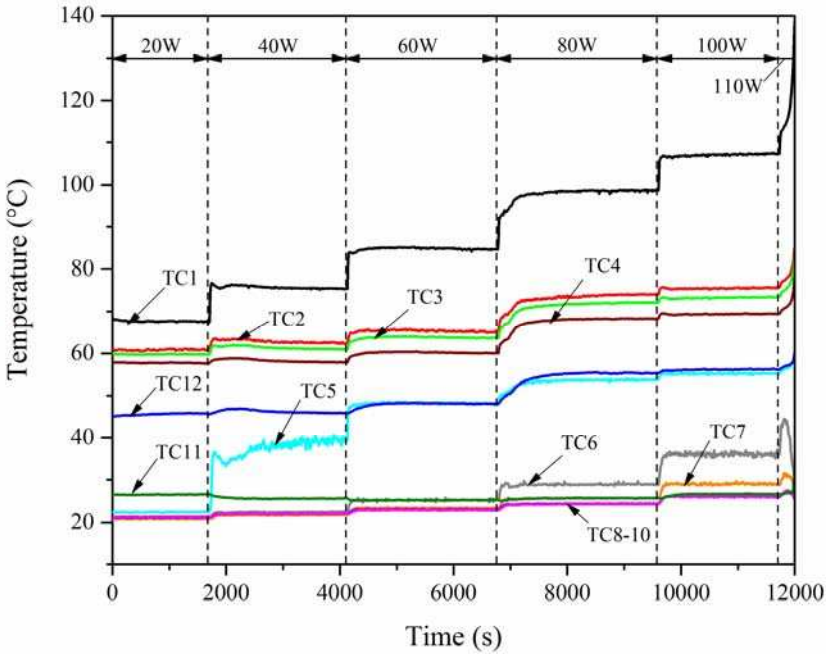

Fig. 11 Heat transfer limit for LHP with 4 mm inner diameter pipeline

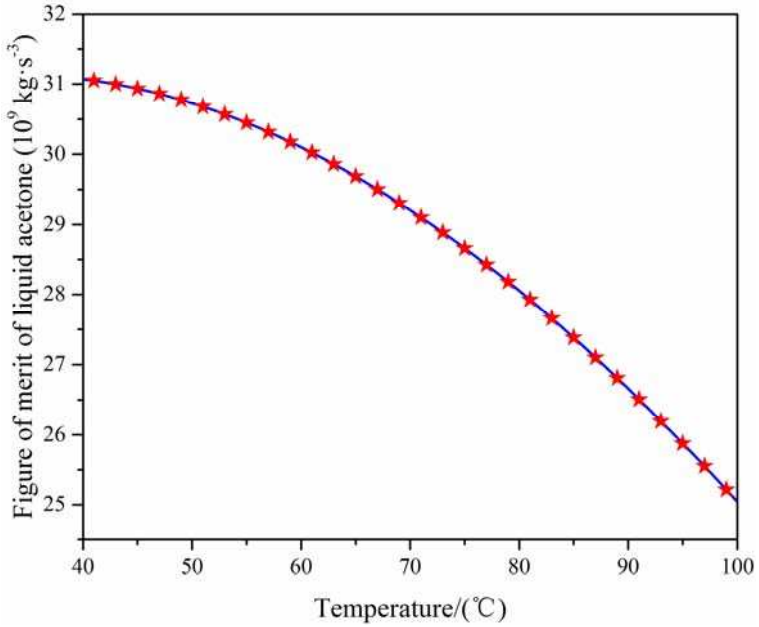

Fig. 12 Temperature dependence of Figure of Merit of liquid acetone

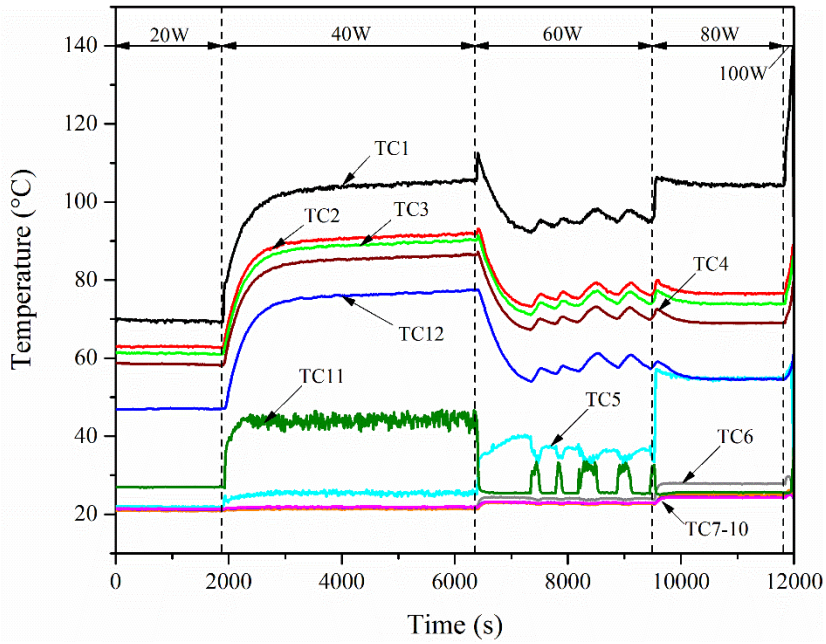

Fig. 13 Heat transfer limit for LHP with 4 mm inner diameter pipeline (0.1 m adverse elevation)

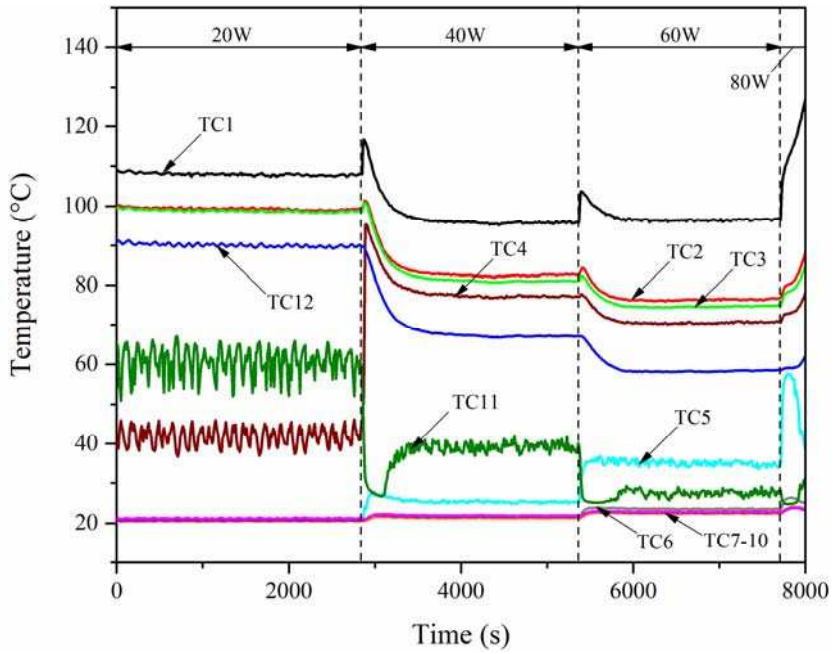

Fig. 14 Heat transfer limit for LHP with 4 mm inner diameter pipeline (0.2 m adverse elevation)